Probing Layer Number and Stacking Order of Few-Layer Graphene by Raman Spectroscopy**

*Yufeng Hao, Yingying Wang, Lei Wang, Zhenhua Ni, Ziqian Wang, Rui Wang, Chee Keong Koo, Zexiang Shen, and John T. L. Thong**

Graphene is a two-dimensional material defined as a planar honeycomb lattice of close-packed carbon atoms, where the electrons exhibit a linear dispersion near Dirac **K** points and behave as massless Dirac fermions.[1,2] However, the valence and conduction bands in an *AB* stacked graphene bilayer split into two parabolic branches near the **K** point originating from the interaction of π electrons, and the electrons are hence described by massive Dirac fermions.[2–4] Moreover, a graphene bilayer is a tunable-gap semiconductor under electric-field biasing.[5] With a further increase in the number of layers along with *AB* stacking, the electronic structure reveals stepwise variations that eventually approach that of the three-dimensional counterpart.[6–8] Considering the close relation between the electronic properties and layer number of few-layer graphene (FLG), the ability to accurately determine the layer number and correlating this with the electronic structure is a prerequisite in understanding the evolution of the electronic properties from two- to three-dimensional graphitic materials. In addition to graphene layers with *AB* stacking, FLG with arbitrary stacking (Figure 1) is considered to possess distinct properties arising from its different crystalline structure and π electron interactions.[9] Experimentally, it has been observed that the electro- and magnetotransport properties for folded graphene sheets are different to those of *AB* stacked bilayers.[10] Furthermore, FLG grown on SiC,[11] Ni,[12–14] and Ru[15] also have non-*AB* stacking order. Therefore, elucidating the detailed characteristics of this type of FLG is required not only for the overall understanding of the structural and electronic properties but also for the development of FLG-based devices.

Raman scattering is a rapid, sensitive, and non-destructive tool for the characterization of carbon-based materials.[16] Furthermore, the phonons in Raman scattering are directly linked to the electronic dispersion of graphitic materials by the well-established double-resonance model, and thus the Raman signals manifest not only lattice vibrations but also the electronic band structure configuration and modifications.[17] During the past two to three years, several pioneering works have been carried out to elucidate the Raman characteristics of graphene, such as differentiating single-layer and bilayer from bulk graphite,[18–20] detecting charge impurities,[21,22] structural defects,[18] edge states (armchair or zigzag),[29,30] strain effects,[23] determining the crystalline orientations,[27,28] and investigating electron–phonon coupling for biased graphene.[24–26]

In this Communication, detailed work is carried out on Raman spectroscopy study of *AB*-stacked FLG: the full width at half-maximum (FWHM) of the 2D band is found to be a quantitative guide to distinguish the layer number (single- to five-layer) of FLG. The splitting of the electronic band structure in FLG is responsible for the stepwise broadening of 2D bands according to the theoretical model of double resonance. Subsequently, folded FLG is taken as an example to investigate the electronic properties of non-*AB* stacked FLG. The consistent blueshift and similarity in shape and FWHM of the 2D band of folded FLG suggest slightly modified electronic energy dispersion curves near the **K** points as well as weak coupling between graphene layers with arbitrary stacking. We emphasize the link between the Raman characteristics and the nature of the interlayer interaction, that is, *AB* stacking and non-*AB* stacking. This research provides a means for fast confirmation of layer number and stacking manner, and sheds insight into the evolution of the electronic band structure for applications in FLG-based electronic devices in the near future.

The main features in Raman spectra of graphite-based materials are the G and D bands and the second order of the D band, so-called 2D, all of which change in shape, position, and relative intensity and thus reflect the evolution of the structural and electronic properties.[31] Figure 2a and d are the optical image and corresponding Raman spectra of a typical FLG from single- to four-layer, respectively. The G band, standing at around 1580 cm^{-1}, refers to optical phonons at the Brillouin

[*] Prof. J. T. L. Thong, Dr. Y. Hao, L. Wang, Z. Wang, R. Wang, C. K. Koo
Center for Integrated Circuit Failure Analysis and Reliability (CICFAR)
Department of Electrical and Computer Engineering
National University of Singapore
117576 (Singapore)
E-mail: elettl@nus.edu.sg
Prof. Z. Shen, Dr. Z. Ni, Y. Wang
Division of Physics and Applied Physics
School of Physical and Mathematical Sciences
Nanyang Technological University
637371 (Singapore)

[**] The authors thank Dr. Ting Yu at Nanyang Technological University and Dr. Minggang Xia at Xi'an Jiaotong University for fruitful discussions. This research was financially supported by A*STAR (Project No. 062 101 0023) and the NRF-CRP grant.

Supporting Information is available on the WWW under http://www.small-journal.com or from the author.

DOI: 10.1002/smll.200901173

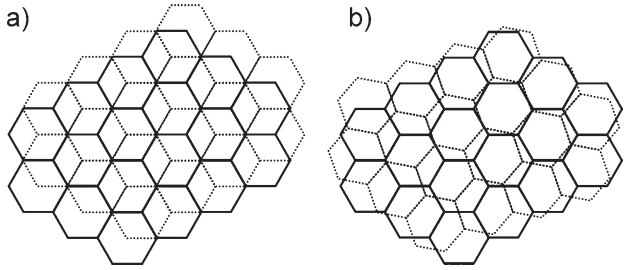

Figure 1. Top view of a pair of graphene lattices with a) *AB* stacking order and b) non-*AB* stacking.

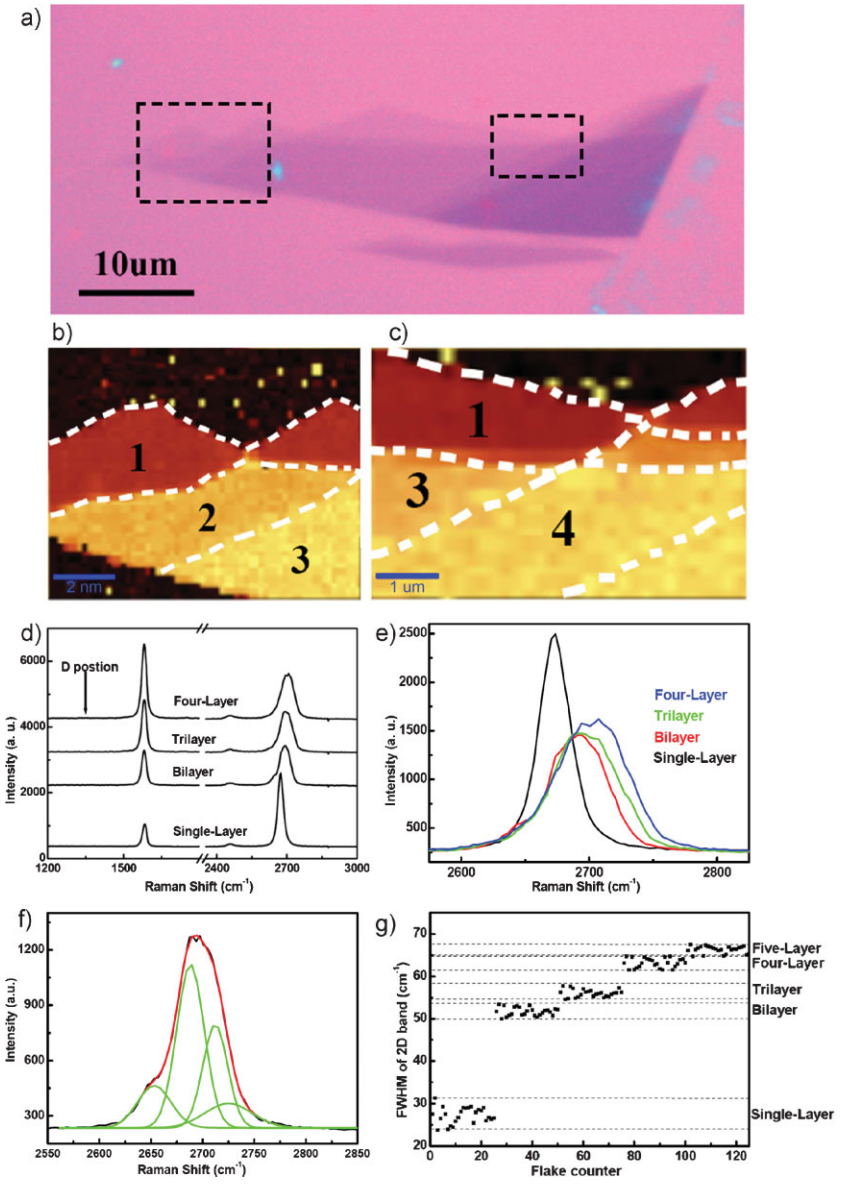

Figure 2. Raman characterizations of *AB*-stacked FLG. a) Optical image of graphene flakes with continuous layer number from 1 to 4. b,c) Raman images from left box and right box in (a), respectively, according to FWHM of 2D band. Brighter color represents larger FWHM of Raman bands. Layer numbers are indicated in each part. Note that, for clarity, the two images are scaled by different brightness. d) Raman spectra of each part of the FLG in (a). e) The 2D bands from (b) are magnified to show different FWHM of each FLG with different layer number. f) The fitted four components of the 2D band in bilayer graphene. The statistical data of FWHM with respect to different layer number is plotted in (g).

zone center Γ point, corresponding to in-plane carbon-atom stretching vibrations. This band becomes more intense with increasing layer number due to more carbon atoms contributing to this vibration mode. However, its intensity, shape, and position are sensitive to any intentionally and unintentionally charged impurities[21,25] or induced strain when fabricating samples.[23,27,28] The positions of the D and 2D band are excitation-energy dependent and occur at around 1350 cm^{-1} and 2700 cm^{-1}, respectively (Figure 2d), under 2.33 eV laser excitation. Both are induced by double-resonance processes that reflect the characteristics of phonon dispersions and electronic band structures around **K** points in the Brillouin zone.[32] Nevertheless, the D band requires defects for its activation, hence, it is absent for perfect crystalline graphene samples, as in the present case from micromechanically cleaved graphite (Figure 2d). The 2D band, on the contrary, always exists even if its first order is absent. Four successive transitions, as shown in Figure 3a, are involved for underlying formation mechanism of the 2D band according to the typical double-resonance model:[18] laser-induced excitation of electron–hole pair (a → b), scattering (b → c, the first resonance process) and back-scattering (c → b, the second resonance process) of the excited electron by two phonons with wave vectors q and $-q$, respectively, and electron–hole pair recombination (b → a). The procedure links two optical phonons near **K** and **K'** points to the electronic band structure, and therefore Raman signals are crucial fingerprints that reflect the electronic band structure evolution in FLG.

As for single-layer graphene (SLG), the 2D band is symmetric and can be fitted into only one Lorentzian peak (Figure 2d and e), which represents the single π electron valence band and π* conduction band structure, and therefore only one Raman scattering cycle is excited near the **K** and **K'** points (Figure 3a). Here, its FWHM is 26.3 cm^{-1}. In bilayer graphene, the interaction of the two graphene planes causes the π and π* electron bands to divide into four parabolic band structures denoted as π_1, π_2, π_1*, and π_2*(Figure 3b). Incident laser light can excite electrons in only two pairs, $\pi_1 \Leftrightarrow \pi_1$* and $\pi_2 \Leftrightarrow \pi_2$*, among the four bands according to space–group theory.[32,33] Two of the four Raman scattering cycles are demonstrated in Figure 3b regarding $\pi_1 \Leftrightarrow \pi_1$*. The 2D band is thus dispersive and fitted into four Lorentzian bands with slightly different frequencies (Figure 2f). The Raman spectrum has a wider FWHM of 52.1 cm^{-1}, about twice that of SLG. In trilayer and four-layer

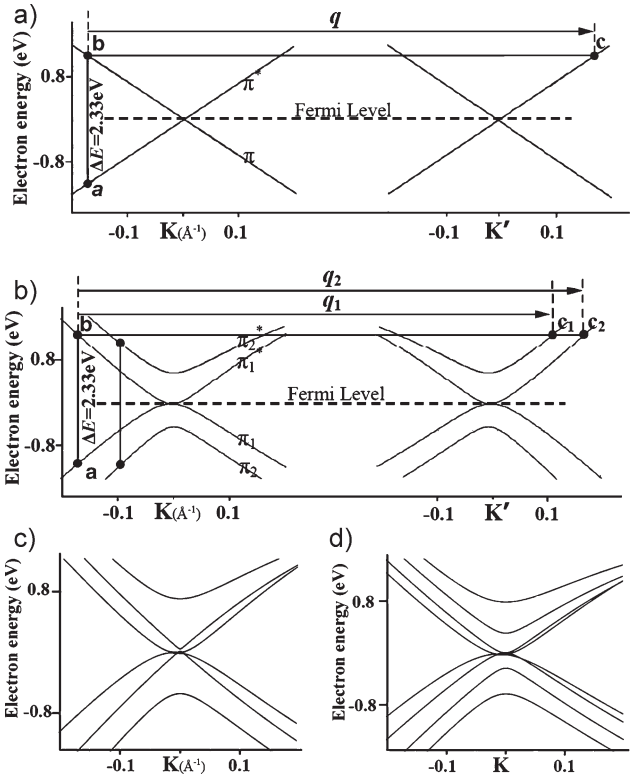

Figure 3. a,b) Electronic band structures and Raman scattering processes of SLG and *AB*-stacked bilayer graphene, respectively.[6,7,18] c,d) Electronic band structures for *AB*-stacked trilayer and four-layer graphene, respectively. The electronic band structures of *AB*-stacked FLG are schematically illustrated from the tight-binding approximation.[6,7]

graphene, the electronic bands split into more complex and dispersive configurations (Figure 3c and d) due to the π electron interactions under *AB* stacking,[7] and therefore excited electron–hole pairs are involved in more scattering cycles, so more resonant phonons with different frequencies contribute to the wider 2D bands. Although the shapes are similar for the 2D bands, there are obvious differences in the FWHM: 56.1 cm^{-1} and 62.4 cm^{-1} for tri- and four-layer graphene, respectively. Furthermore, Raman images based on the FWHM of 2D bands (Figure 2b and c) unambiguously show the difference in brightness according to the layer number, in correspondence with the contrast in the optical image of this FLG from single-layer to four-layer graphene. After characterizations of a large number of *AB*-stacked FLG samples during the past year, the typical FWHM of 2D peaks of various FLGs are plotted in Figure 2g. It is clear that there are consistent, substantial, and distinguishable ranges for single-, bi-, tri-, four-, and five-layer graphene at $27.5 \pm 3.8\,cm^{-1}$, $51.7 \pm 1.7\,cm^{-1}$, $56.2 \pm 1.6\,cm^{-1}$, $63.1 \pm 1.6\,cm^{-1}$, and $66.1 \pm 1.4\,cm^{-1}$, respectively. Furthermore, there is no overlap for different thicknesses of FLG, and therefore the data can be a straightforward standard for determining the number of layers. The statistical ranges of the 2D band FWHM reflect the stepwise evolution of the electronic band structure of the *AB*-stacked FLG at room temperature, and provide quantitative fingerprints to distinguish the layer number of FLG on SiO_2/Si substrate. It is noted that, unlike 2D band positions and intensity, the FWHM is less affected by excitation energy,[32] charge impurity,[21,22] and so on.

For FLG thicker than five layers, the Raman spectrum is hardly distinguishable from that of bulk graphite as continuous splitting of valence and conduction bands leads to the 2D band approaching that of bulk graphite.[18,31] To this end, the multicomponent and stepwise evolution of 2D bands in FLG has been found to be a good indication of *AB* stacking, and suggests strong coupling of conducting electrons for such stacking. A point to mention here is that the integrated intensity of the 2D bands is similar (Figure 2e) for *AB*-stacked FLG with a different layer number under identical excitation conditions.[19,34] This is distinct from misoriented FLG, as discussed below.

Folded FLG is normally formed with arbitrary orientation by post-treatment and is a fair example to probe the changes in the electronic properties induced by non-*AB* stacking (Figure 1b). The optical images, taken before and after folding of a bilayer graphene in Figure 4a and b, respectively, clearly show where the folding occurs. The Raman spectra of the unfolded and folded parts of this sample, and another *AB*-stacked four-layer graphene, which is used for comparison, are presented in Figure 4e, all of which were measured under the same experimental conditions. It is observed from the Raman spectra that the 2D band of the folded part blueshifts 4.8 cm^{-1} compared to that of its corresponding bilayer. Furthermore, the integrated intensity of the 2D band of the folded part turns in at around twice that of the bilayer and four-layer graphene (Figure 4f), unlike that for *AB*-stacked FLG, where the integrated intensity is about the same, irrespective of the layer number. However, the FWHM of the 2D band of the folded part, 52.1 cm^{-1}, is similar to that of the bilayer graphene, 52.9 cm^{-1}, and these values are substantially narrower than that of four-layer graphene at ≈64 cm^{-1}. On the other hand, the G band integrated intensity and position of the folded part, as expected, are similar to that for *AB*-stacked four-layer since both of them contain four layers of graphene sheets. In addition, no obvious position shift is observed in the G band. In Figure 4c and d, Raman images further confirmed the uniform distributions of these Raman features on the folded and unfolded parts. In this work, a total of three folded bilayer graphene samples were measured, and blueshift (≈4.8, 7.1, and 8.1 cm^{-1}) and a much higher integrated intensity of 2D bands were invariably observed. However, the FWHM of the 2D band is either slightly bigger or smaller (±2 cm^{-1}) than that of bilayer graphene without a consistent pattern. We further measured the Raman spectra of three folded five-layer graphene samples, as shown in Figure 4g, and still found, for folded samples, both 2D band blueshift (2.9, 2.3, and 1.8 cm^{-1}) and integrated intensity around 1.5 times greater than that for the *AB*-stacked five-layer graphene, but the variation is smaller compared to the folded bilayer case. In addition, the FWHM of 2D bands are similar between the folded and the unfolded five-layer samples. Therefore, the 2D band FWHM-based evaluation of layer number remains valid only for *AB*-stacked FLG.[35]

Due to deviation from *AB* stacking, the π electron interactions between graphene layers generally exhibit different features and evolution rules from *AB*-stacked FLG.[36] Previous theoretical calculations have shown that misoriented

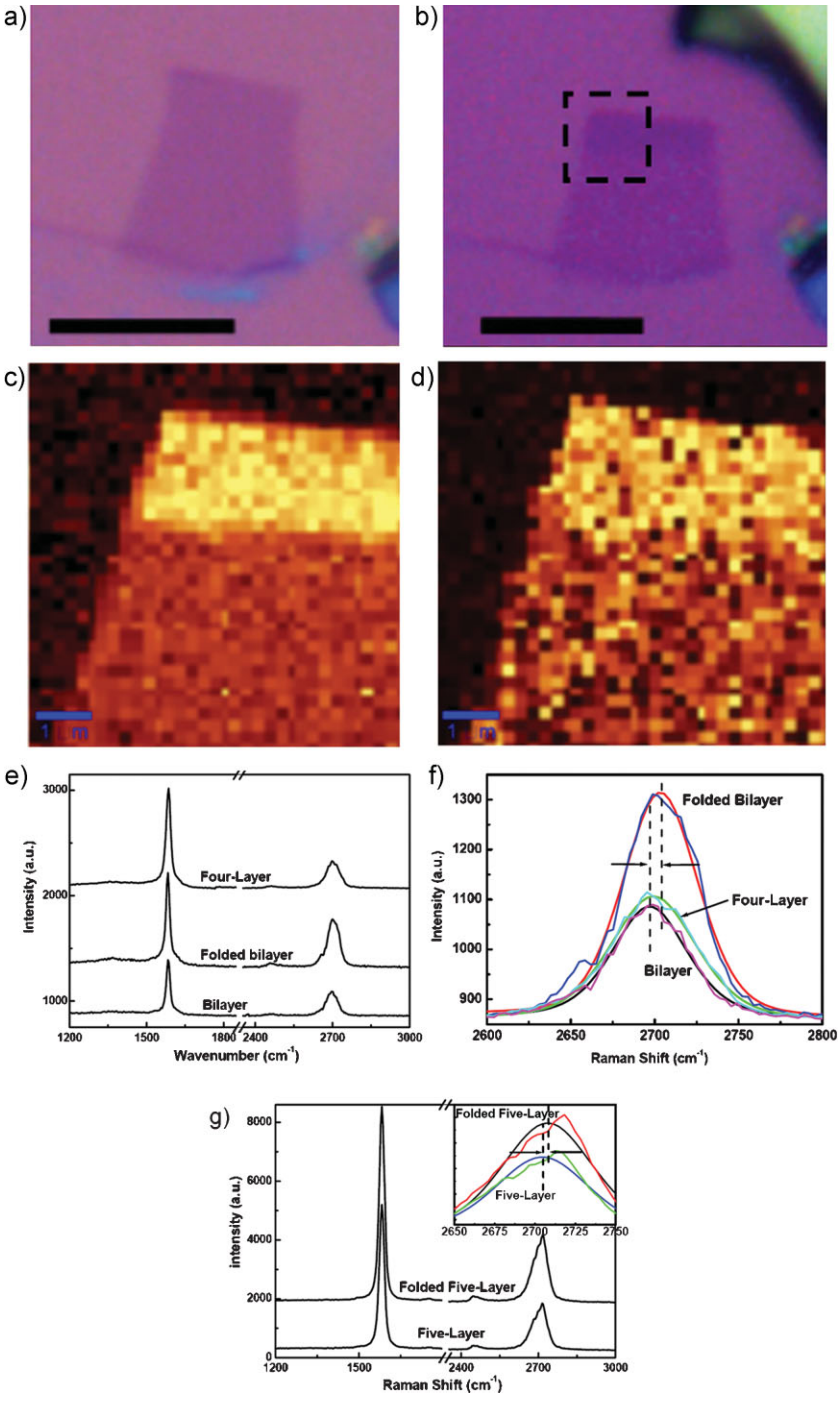

Figure 4. Raman characterizations of folded FLG. a,b) Optical images of bilayer graphene before and after folding, respectively. The scale bar is 5 μm. c,d) Raman images of the folded parts, taken from the dashed box in (b), according to the 2D band integrated intensity and 2D band position, respectively. Brighter color represents higher intensity and higher wave number of Raman scattering, respectively. The Raman spectra from the unfolded and folded parts of this sample and another *AB*-stacked four-layer graphene are shown in (e). f) The 2D bands from (e) are highlighted to show the variations after folding. Lorentzian fittings are used to calculate the blueshift quantity between bilayer and folded bilayer. g) Raman spectra of unfolded and folded parts of a five-layer graphene; the inset in (g) shows the highlighted 2D band parts. Blueshift can be observed in fitted 2D peaks.

graphene bilayers exhibit electronic structures that are similar to those of SLG but with reduced Fermi velocity, that is, a smaller slope of electronic band near the **K** points.[9] However, the *AB*-stacked FLG has more sub-bands originating from interlayer interactions, as shown in Figure 3, and after folding should exhibit more complicated variations, that is, similar FWHM, stronger integrated intensity, and blueshift of the 2D bands. In contrast to the layer number-related 2D band broadening in *AB*-stacked FLG, the similar FWHM between the folded and the unfolded regions indicates that the electronic bands in the folded FLG did not split into more branches around **K** points.[37] Whereas, it is considered that the two 2D bands from the folded structures superpose with each other, giving rise to nearly doubling of the integrated intensity, and therefore suggesting weak interactions of π electrons between the two parts that form the folded FLG structures. With regard to the blueshift, for simplicity, we still consider linear π electron bands to elucidate the Raman scattering processes, as shown in Figure 5. For a specific laser excitation energy (2.33 eV in this work), the phonon with larger wave vector q' couples the Raman process that corresponds to a reduced slope of electronic sub-bands. Considering the nearly linear phonon frequency–wave vector dispersion (ω–q) of graphite near **K** point, higher frequency ω contributes to the 2D band.[31] This just reflects the smaller slope and reduced Fermi velocity of at least some sub-bands in electronic energy dispersion near the **K** points, as it is difficult for Raman spectra to detect the exact variations/configurations of every sub-band after folding. In this way, the folded FLG always shows similar Raman characteristics, suggesting that the electronic structure is slightly modified, corroborates our previous study on folded SLG,[34,38] and further extends the conclusions to folded FLG. We also fitted the 2D bands of the folded bilayer into four components similar to that of bilayer graphene, and found coincidently similar relative weights of these components (not shown here) as those of bilayer. This provides confirmation that the blueshift of the 2D bands did not arise from changes in the relative weights of the four components.

From the Raman characteristics, we found that the G band is unchanged, which means the phonons at Γ points are untouched. The folded parts, around tens

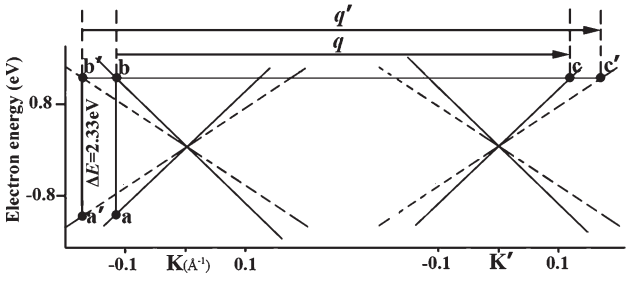

Figure 5. Schematic illustration of certain sub-band electronic structures of FLG (solid line), folded FLG (dashed line), and the corresponding double-resonant Raman scattering processes.

of micrometers[2] in size, should not induce obvious lattice distortion/tension. Therefore, the phonon dispersion in folded FLG may be almost unchanged. It is also noted that Poncharal et al. proposed that the blueshift of the 2D band in misoriented FLG may come from a modified phonon dispersion curve.[39–41] This is different to the finding in our work. Further investigation using other characterization methods might be required for the exact origin of the blueshift in the 2D band. In addition, molecules such as water, oxygen, or nitrogen may be trapped in the folded FLG during sample fabrication, and hence hinder the interactions between the two pieces. However, Raman characteristics did not show any detectable variations upon annealing that may expel the trapped molecules in the folded FLG. It is also found, from atomic force microscopy (AFM) measurements, that the thickness of annealed folded FLG stays almost the same as that before annealing. Therefore, the trapped molecules should not have any effect on the observed Raman features of the folded FLG.

In summary, phenomenal observations in conjunction with physical interpretation were used to present an overall scenario for Raman scattering spectra of FLG with different stacking geometry. The FWHM, position, and integrated intensity of 2D bands of two types of FLG are found to be informative indices to investigate various features of FLG from the angle of electronic structure variations. Our work will provide a route to discriminate the layer number of *AB*-stacked FLG and yield insight into the features of the electronic structure of folded FLG, and facilitate the use of FLG in various electronic devices.

Experimental Section

The FLG samples were fabricated by micromechanical cleavage of highly oriented pyrolytic graphite (HOPG, Grade SPI-1, SPI Supplies) or natural graphite (NGS Naturgraphit GmbH)[42] and then transferred onto sSilicon substrates covered with a 285-nm thermal oxide layer. It is worth noting that the two types of graphite adopt *AB*-stacking order, which is the stable phase for graphite crystals. FLG samples from the two types of raw material also show almost the same quality with respect to Raman measurements. For investigations of *AB*-stacking-related characteristics, no post-treatments were carried out for the as-prepared samples before Raman measurements. The folded graphene samples were made by gently flushing the graphene sample with water flow. Before Raman measurements, the FLG sheets were characterized by color contrast under optical microscopy[43] and also by AFM topographic measurements to determine the layer number. Annealing treatments for the folded FLG were carried out in a rubber O-ring sealed tube furnace (Blue M Mini-Mite, Lindberg). The experiments are carried out at 450 °C for 2 hours, 5% hydrogen mixed in argon as carrier gas, and tube pressure maintained at 0.1 Torr.

Raman imaging and spectroscopy were carried out on a WITec CRM200 Raman system with 532-nm (2.33 eV) excitation and laser power at the sample below 0.1 mW to avoid laser-induced heating. A 100× objective lens with a numerical aperture (N.A.) = 0.95 was used in the Raman experiments. To obtain the Raman mapping images, a piezo-stage was used to move the sample with a step size of 200 nm and the Raman spectrum was recorded at every point. The stage movement and data acquisition were controlled using ScanCtrl Spectroscopy Plus software from WITec GmbH, Germany. Data analysis was carried out using WITec Project software.

Keywords:

electronic structure · graphene · Raman spectroscopy · stacking

[1] K. S. Novoselov, A. K. Geim, S. M. Morozov, M. I. Katsnelson, I. V. Grigorieva, S. V. Dubonos, A. A. Firsov, *Nature* **2005**, *438*, 197.
[2] A. K. Geim, K. S. Novoselov, *Nat. Mater.* **2007**, *6*, 183.
[3] E. V. Castro, K. S. Novoselov, S. V. Morozov, N. M. R. Peres, J. M. B. Lopes dos Santos, J. Nilsson, F. Guinea, A. K. Geim, A. H. Castro Neto, *Phys. Rev. Lett.* **2007**, *99*, 216802.
[4] T. Ohta, A. Bostwick, T. Seyller, K. Horn, E. Rotenberg, *Science* **2006**, *313*, 951.
[5] Y. B. Zhang, T. T. Tang, C. Girit, Z. Hao, M. C. Martin, A. Zettl, M. F. Crommie, Y. R. Shen, F. Wang, *Nature* **2009**, *459*, 820.
[6] B. Partoens, F. M. Peeters, *Phys. Rev. B* **2006**, *74*, 075404.
[7] A. Grüneis, C. Attaccalite, L. Wirtz, H. Shiozawa, R. Saito, T. Pichler, A. Rubio, *Phys. Rev. B* **2008**, *78*, 205425.
[8] M. F. Craciun, S. Russo, M. Yamamoto, J. B. Oostinga, A. F. Morpurgo, S. Tarucha, *Nat. Nanotech.* **2009**, *4*, 383.
[9] J. M. B. Lopes dos Santos, N. M. R. Peres, A. H. Castro Neto, *Phys. Rev. Lett.* **2007**, *99*, 256802.
[10] H. Schmidt, T. Lüdtke, P. Barthold, E. McCann, V. I. Fal'ko, R. J. Haug, *Appl. Phys. Lett.* **2008**, *93*, 172108.
[11] J. Hass, F. Varchon, J. E. Millán-Otoya, M. Sprinkle, N. Sharma, W. A. de Heer, C. Berger, P. N. First, L. Magaud, E. H. Conrad, *Phys. Rev. Lett.* **2008**, *100*, 125504.
[12] A. Reina, X. Jia, J. Ho, D. Nezich, H. Son, V. Bulovic, M. S. Dresselhaus, J. Kong, *Nano Lett.* **2009**, *9*, 30.
[13] K. S. Kim, Y. Zhao, H. Jang, S. Y. Lee, J. M. Kim, K. S. Kim, J. H. Ahn, P. Kim, J. Y. Choi, B. H. Hong, *Nature* **2009**, *457*, 706.
[14] Q. K. Yu, J. Lian, S. Siriponglert, H. Li, Y. P. Chen, S. S. Pei, *Appl. Phys. Lett.* **2008**, *93*, 113103.
[15] P. W. Sutter, J. Flege, E. A. Sutter, *Nat. Mater.* **2008**, *7*, 406.
[16] A. C. Ferrari, J. Robertson, *Phil. Trans. R. Soc. A* **2004**, *362*, 2267.
[17] C. Thomsen, S. Reich, *Phys. Rev. Lett.* **2000**, *85*, 5214.
[18] A. C. Ferrari, J. C. Meyer, V. Scardaci, C. Casiraghi, M. Lazzeri, F. Mauri, S. Piscanec, D. Jiang, K. S. Novoselov, S. Roth, A. K. Geim, *Phys. Rev. Lett.* **2006**, *97*, 187401.
[19] D. Graf, F. Molitor, K. Ensslin, C. Stampfer, A. Jungen, C. Hierold, L. Wirtz, *Nano Lett.* **2007**, *7*, 238.
[20] A. Gupta, G. Chen, P. Joshi, S. Tadigadapa, P. C. Eklund, *Nano Lett.* **2006**, *6*, 2667.
[21] Z. H. Ni, T. Yu, Z. Q. Luo, Y. Y. Wang, L. Liu, C. P. Wong, J. M. Miao, W. Huang, Z. X. Shen, *ACS Nano* **2009**, *3*, 569.

[22] C. Casiraghi, S. Pisana, K. S. Novoselov, A. K. Geim, A. C. Ferrari, *Appl. Phys. Lett.* **2007**, *91*, 233108.
[23] T. Yu, Z. H. Ni, C. L. Du, Y. M. You, Y. Y. Wang, Z. X. Shen, *J. Phys. Chem. C* **2008**, *112*, 12602.
[24] L. M. Malard, D. C. Elias, E. S. Alves, M. A. Pimenta, *Phys. Rev. Lett.* **2008**, *101*, 257401.
[25] A. Das, S. Pisana, B. Chakraborty, S. Piscanec, S. K. Saha, U. V. Waghmare, K. S. Novoselov, H. R. Krishnamurthy, A. K. Geim, A. C. Ferrari, A. K. Sood, *Nat. Nanotech.* **2008**, *3*, 210.
[26] J. Yan, Y. B. Zhang, P. Kim, A. Pinczuk, *Phys. Rev. Lett.* **2007**, *98*, 166802.
[27] M. Y. Huang, H. G. Yan, C. Y. Chen, D. H. Song, T. F. Heinz, J. Hone, *Proc. Natl. Acad. Sci. USA* **2009**, *106*, 7304–7308.
[28] T. M. G. Mohiuddin, A. Lombardo, R. R. Nair, A. Bonetti, G. Savini, R. Jalil, N. Bonini, D. M. Basko, C. Galiotis, N. Marzari, K. S. Novoselov, A. K. Geim, A. C. Ferrari, *Phys. Rev. B* **2009**, *79*, 205433.
[29] C. Casiraghi, A. Hartschuh, H. Qian, S. Piscanec, C. Georgi, A. Fasoli, K. S. Novoselov, D. M. Basko, A. C. Ferrari, *Nano Lett.* **2009**, *9*, 1433.
[30] Y. M. You, Z. H. Ni, T. Yu, Z. X. Shen, *Appl. Phys. Lett.* **2008**, *93*, 163112.
[31] A. C. Ferrari, *Solid State Commun.* **2007**, *143*, 47.
[32] L. M. Malard, J. Nilsson, D. C. Elias, J. C. Brant, F. Plentz, E. S. Alves, A. H. Castro Neto, M. A. Pimenta, *Phys. Rev. B* **2007**, *76*, 201401.
[33] L. G. Cançado, A. Reina, J. Kong, M. S. Dresselhaus, *Phys. Rev. B* **2008**, *77*, 245408.
[34] Z. H. Ni, Y. Y. Wang, T. Yu, Y. M. You, Z. X. Shen, *Phys. Rev. B* **2008**, *77*, 235403.
[35] S. Latil, V. Meunier, L. Henrard, *Phys. Rev. B* **2007**, *76*, 201402.
[36] M. A. Pimenta, G. Dresselhaus, M. S. Dresselhaus, L. G. Cancado, A. Jorio, R. Saito, *Phys. Chem. Chem. Phys.* **2007**, *9*, 1276.
[37] Recently, we found that, as for folded graphene, the electronic band splits close to **M** point of Broullion zone, while the electronic band structures around **K** points remain unchanged. A related paper is to be published elsewhere.
[38] Z. H. Ni, Y. Y. Wang, T. Yu, Y. M. You, Z. X. Shen, *Phys. Rev. B* **2009**, *79*, 237401.
[39] P. Poncharal, A. Ayari, T. Michel, J.-L. Sauvajol, *Phys. Rev. B* **2008**, *78*, 113407.
[40] P. Poncharal, A. Ayari, T. Michel, J.-L. Sauvajol, *Phys. Rev. B* **2009**, *79*, 195417.
[41] P. Poncharal, A. Ayari, T. Michel, J.-L. Sauvajol, *Phys. Rev. B* **2009**, *79*, 237402.
[42] K. S. Novoselov, D. Jiang, F. Schedin, T. J. Booth, V. V. Khotkevich, S. V. Morozov, A. K. Geim, *Proc. Natl. Acad. Sci. USA* **2005**, *102*, 10451.
[43] Z. H. Ni, H. M. Wang, J. Kasim, H. M. Fan, T. Yu, Y. H. Wu, Y. P. Feng, Z. X. Shen, *Nano Lett.* **2007**, *7*, 2758.

Received: July 6, 2009
Revised: September 5, 2009
Published online: November 11, 2009

